Direct-Reading One-Port Acoustic Network Analyzer*

C. M. DE BLOK AND R. F. M. VAN DEN BRINK

PTT Research, 2260 AK Leidschendam, The Netherlands

A novel measurement instrument is proposed to perform reflection measurements of guided acoustic waves. Both the magnitude and the phase of the reflection coefficient are measured simultaneously. The compact construction and the direct-readout feature facilitate an attractive measurement alternative for traditional standing-wave-ratio (SWR) detectors with movable microphones. These advantages are decisive for infrasonic frequencies where traditional SWR detectors require setups of 10 m or more.

0 INTRODUCTION

In a recent publication [1] acoustic one-ports and two-ports were introduced to facilitate a full description of (segments of) a closed linear acoustic system, including an instrument to measure these N-port parameters. Reflection measurements were performed with traditional standing-wave detection methods [2], which implies that the locations of the minima and the maxima were detected by manual adjustment of the positions of movable microphones. The disadvantages of this method are that 1) reflection measurements are laborious, 2) the method is based on movable microphones and therefore not suitable for real-time measurements, and 3) the minimum instrument length must exceed one-half the longest wavelength of interest. While infrasonic standing-wave-ratio (SWR) measurement instruments would require a minimum length of 35 m below 5 Hz, the length of the instrument proposed here is irrelevant and can be kept below 0.2 m.

Alternative methods, using two or more fixed microphones, are known from the literature. In [5] a measurement setup is described based on a loss-free acoustic wave guide and two wall-mounted microphones. Because the reflection is a function of spatial difference in pressure, a computer was used for the reconstruction of the reflection coefficient. The low end of this frequency range is limited by the accuracy with which the minimum phase difference can be detected. In [5] reflection measurements are reported using an offset distance of 0.13 m, with a usable frequency range from 100 Hz to 3.6 kHz. At the lowest frequency, the phase difference of the reported setup has been reduced to 13.6° in the case of traveling waves. Down scaling the measurement setup to 1 Hz with the same accuracy would require a microphone offset distance of at least 13 m.

We propose an improved one-port network analyzer (NWA) to measure acoustic reflections in regular tubes. The method proposed here is also based on two fixed microphones, but separates the microphones by an acoustic attenuator instead of a loss-free transmission line. Next, the microphone signals are interfered in a virtual bridge circuit to generate two related signals. As a result, the reflection coefficient in magnitude and phase has become linear proportional to the ratio of the two signals. Signal processing in a computer is not required, because magnitude and phase are directly measurable with, for example, an oscilloscope (using Lissajous figures).

The overall instrument length is remarkably short, compared to the longest wavelength of interest. The lowest usable frequency is limited mainly by the performance of the loudspeaker and microphones, and not restricted by the distance between the two microphones. The highest usable frequency is limited by the tube diameter [2] and the internal construction. Below that frequency limit the propagation of plane waves is guaranteed. The usable frequency band of the experimental setup ranges from 1 Hz to 100 Hz and is therefore useful for measurements on, for example, loudspeaker cabinets and tubes of air conditioning systems.

1 BASIC PRINCIPLE

The reflection of guided acoustic waves in a tube to obstacles and irregularities is fully related to the associated acoustic impedance. The equivalent input impedance Z_x of such a set of obstacles, observed at a

* Manuscript received 1992 July 6; revised 1993 February 2.

well-defined reference plane [1], is defined as the quotient of the complex transformed representation of the average sound pressure p and the volume flow rate u at that reference plane. When this impedance is not equal to the characteristic impedance $\mathbb{Z}_0$ of the tube, the reference plane will pass both incident (ψ^+) and reflected (ψ^-) waves. Following the definition[1] of acoustic plane waves through this reference plane in its complex transformed form [1], the relation between impedance Z_x and reflection coefficient $\Gamma_x = (\psi^-/\psi^+)$ can be derived as follows:

$$\psi^+ = \tfrac{1}{2}\sqrt{\mathbb{Z}_0}\left(\frac{p}{\mathbb{Z}_0} + u\right)$$

$$\psi^- = \Gamma_x \cdot \psi^+ = \tfrac{1}{2}\sqrt{\mathbb{Z}_0} \cdot \left(\frac{p}{\mathbb{Z}_0} - u\right) .$$

Then

$$\Gamma_x = \frac{\psi^-}{\psi^+} = \frac{p/\mathbb{Z}_0 - u}{p/\mathbb{Z}_0 + u} = \frac{p/u - \mathbb{Z}_0}{p/u + \mathbb{Z}_0} = \frac{Z_x - \mathbb{Z}_0}{Z_x + \mathbb{Z}_0} .$$

Due to this relation between Γ_x and Z_x, reflection measurements on one-port networks can be obtained from impedance measurements and do not necessarily require the detection of standing waves.

A simple way to measure an impedance is the detection of the drop in sound pressure over an acoustic impedance in series with the impedance of interest. Fig. 1 shows the basic setup of such a measurement, in which the series impedance is realized with absorbing material. Two fixed microphones sense the sound pressure and generate sinusoidal voltages with associated complex transformed values U_s and U_t. The voltage drop $U_s - U_t$, which is proportional to the sound pressure, will be maximum when the acoustic network analyzer is terminated by an open end ($Z_x = 0$; $\Gamma_x = -1$) and minimum in the case of a covered end ($Z_x = \infty$; $\Gamma_x = +1$).

Fig. 2 shows the equivalent electric circuit model of the acoustic network analyzer of Fig. 1. The impedance Z_x is defined as the ratio of voltage to current in their complex transformed forms. This ratio is equivalent to the following ratio between the microphones voltages U_s and U_t:

$$U_s = \frac{Z_s + Z_x}{Z_{ss} + Z_s + Z_x} * U_{ss}$$

$$U_t = \frac{Z_x}{Z_{ss} + Z_s + Z_x} * U_{ss} .$$

Hence,

$$Z_x = \frac{U_t}{U_s - U_t} * Z_s .$$

The reflection coefficient Γ_x is defined as the ratio of incident wave to reflected wave in their complex transformed forms. Similar to impedance, this ratio can be transformed into a ratio of microphone voltages. For that purpose we define the quantities "reflective" voltage U_r and "reference" voltage U_{ref} as the following combination of U_s and U_t:

$$U_r = -\left(U_s - \frac{\mathbb{Z}_0 + Z_s}{\mathbb{Z}_0} \cdot U_t\right)$$

$$= \frac{Z_x - \mathbb{Z}_0}{Z_{ss} + Z_s + Z_x} * \left(\frac{Z_s}{\mathbb{Z}_0} * U_{ss}\right)$$

$$U_{ref} = +\left(U_s - \frac{\mathbb{Z}_0 - Z_s}{\mathbb{Z}_0} \cdot U_t\right)$$

$$= \frac{Z_x + \mathbb{Z}_0}{Z_{ss} + Z_s + Z_x} * \left(\frac{Z_s}{\mathbb{Z}_0} * U_{ss}\right) .$$

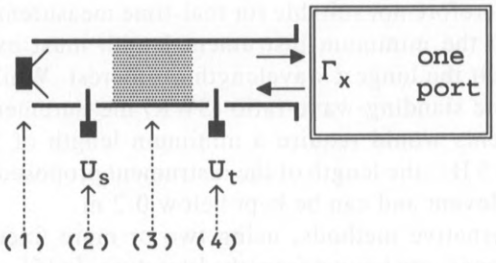

Fig. 1. Basic setup of proposed one-port acoustic network analyzer for measurement of reflection coefficient Γ_x. 1—loudspeaker; 2—first microphone producing voltage U_s; 3—series absorber; 4—second microphone producing voltage U_t.

[1] In the definitions for ψ^+ and ψ^- specified in [1], unfortunately, we neglected to scale ψ with a factor (½), which did not affect the conclusions in [1]. In microwave electronics this scaling factor was added to simplify various power relations. For compatibility, we use the correct definitions here.

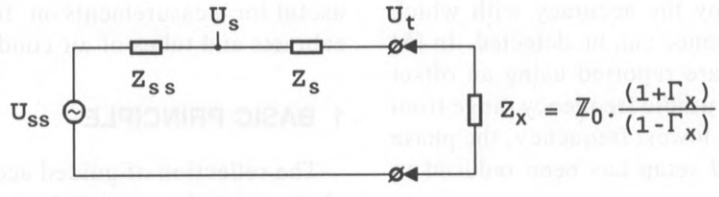

Fig. 2. Equivalent electric circuit model of acoustic network analyzer. Loudspeaker is modeled by voltage source U_{ss} with internal impedance Z_{ss}, serial absorber by impedance Z_s, and reflective load by Z_x. Internal voltages U_s and U_t represent sound pressure detected by microphones.

Then

$$\Gamma_x = \frac{Z_x - \mathbb{Z}_0}{Z_x + \mathbb{Z}_0} = \frac{U_r}{U_{ref}} .$$

Both the reflective voltage and the reference voltage can be made available by means of simple electronic circuits. The amplitude ratio and the phase difference between these two sinusoidal voltages yield the modulus and the phase of Γ_x and are real-time measurable. A simple alternative to the use of phase difference and voltage ratio meters is the use of an oscilloscope to display elliptic Lissajous figures with these two sinusoidal voltages. Fig. 3 illustrates a practical implementation of the network analyzer.

2 PRACTICAL IMPLEMENTATION OF NETWORK ANALYZER

2.1 Impedance Matching

When the overall size of the measurement setup is small compared to the acoustic wavelength of interest, the impedance value of the series absorber is not restricted to a special value. In practical situations the one-port under test is connected to the network analyzer with a tube, and this tube will form a cavity with distinct resonating frequencies. The multiple reflections in this cavity will reduce the measurement accuracy for frequencies close to resonance.

Multiple reflections are avoided when reflected waves are fully absorbed in the network analyzer. This requires the sum of absorber and loudspeaker impedance $Z_s + Z_{ss}$ to be close to the characteristic impedance $\mathbb{Z}_0$ of the tube (matched network analyzer).

2.2 Loudspeaker

Although the loudspeaker choice is not critical, the dynamic range of the cone deflation is preferred to be greater than 5 mm to facilitate the generation of sufficient sound pressure at infrasonic frequencies. As will be demonstrated in Section 3.3, the acoustic loudspeaker impedance is influenced both by the electrical output impedance of the associated amplifier and by the acoustic impedance at the back end of the loudspeaker. This acoustic impedance Z_{ss} should preferably be small compared to the characteristic tube impedance $\mathbb{Z}_0$ to improve a wide-band match of $Z_s + Z_{ss}$ to $\mathbb{Z}_0$ and to increase the overall sensitivity of the instrument. The lowest values for Z_{ss} will be achieved when the electrical output impedance is relatively high and the back end of the loudspeaker is left open. In the experimental setup an 8-Ω loudspeaker (Philips AD5060/W8) was used and driven from a current source.

2.3 Construction of Series Absorber

The series absorber impedance Z_s should preferably be equal to $\mathbb{Z}_0 - Z_{ss}$ to realize a matched network analyzer. In the experimental setup it was realized with polyester wool packed in layers, compressed homogeneously between two perforated metal plates. The density (number of layers) was adjusted empirically within 5% in combination with the loudspeaker by means of standing-wave measurements to meet the matching requirements. It is important that this adjustment be performed with the loudspeaker amplifier activated and at midband frequencies as the acoustic loudspeaker impedance is affected by the amplifier output impedance and the overall acoustic impedance is (slightly) frequency dependent.

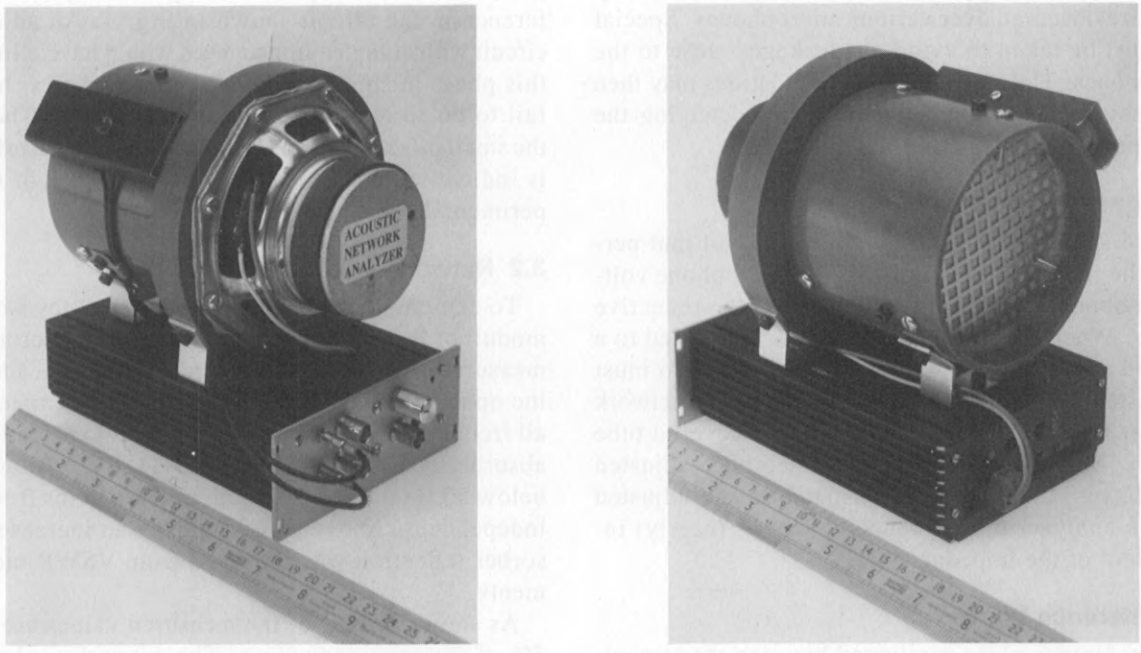

(a) (b)

Fig. 3. Network analyzer. (a) Back view. (b) Front view.

2.4 Dimension of Series Absorber

The required quantity of absorbing material is, roughly, fully related to the required flow resistance Z_s and slightly affected by the absorber length. On the one hand this length must be kept at a minimum to minimize the sound delay time between its end faces and thus to keep the imaginary part of the impedance Z_s as low as possible. On the other hand its length must be maximum to keep the density of the wool low and thus to avoid nonlinear effects. The gas flow in the absorber will become turbulent when the gas velocity around the fibers exceeds a value that depends on the construction and the material. Above this value the flow resistance becomes dependent on the average gas velocity. (See [3], [4] and Section 3.4.)

In the experimental setup a 60-mm series absorber in a 110-mm tube resulted in a 4.6° phase difference at 50 Hz, which is equivalent to 88-mm virtual absorber length. It is plausible that this virtual length increase is mainly caused by a reduction in average velocity due to isothermal propagation [2]. The rest is assumed to be caused by inductive end effects at the transitions air–absorber and absorber–air. For perfect isothermal propagation the velocity reduces to $c = c_0/\sqrt{\gamma} = c_0/\sqrt{1.41}$, which accounts for 80% of the virtual length. In this expression c_0 is the sound velocity in free air and $\gamma = C_p/C_v$ is the ratio of heat capacity at constant pressure to heat capacity at constant volume [2]. (For air, $c_0 = 345$ m/s and $\gamma = 1.41$.)

2.5 Microphones

In the experimental setup low-cost piezoelectric earphones were used on account of their good wide dynamic range, their stability of sensitivity after mechanical shocks, and their convenient packaging. In the range of 1 to 500 Hz a good phase match and a fair sensitivity match are observed over various microphones. Special care must be taken to avoid gas leakages close to the microphones. The associated gas turbulations may then cause severe distortion problems when detecting the sound pressure.

2.6 Signal Preprocessing

Fig. 4 shows a practical electronic circuit that performs the required subtraction of the microphone voltages to obtain the reference voltage and the reflective voltage. When the network analyzer is connected to a matched absorber ($Z_x = \mathbb{Z}_0$), the potentiometer α must be adjusted to minimize the signal U_r. When the network analyzer is subsequently connected to a covered tube aperture ($Z_x = \infty$), then the potentiometer β is adjusted to let $U_{ref} = U_r$. In a properly matched and adjusted network analyzer the reference voltage is (nearly) independent of the impedance Z_x.

2.7 Reference Plane

The reference plane is situated between the two microphones. Their mutual distance is therefore indicative of the phase measurement accuracy. When the network analyzer is extended with various adapters to match various tube diameters, a virtual shift of the reference plane can be achieved by an electrical phase shift of the reflective voltage.

3 EXPERIMENTAL RESULTS

3.1 Reflections to Open, Cover, and Absorber

Fig. 5 shows a set of measured reflection coefficients on various special one-ports at 50 Hz. The theoretical reflections of 1) an open tube end, 2) a covered tube end, and 3) a matched absorber at a distance x from the reference plane have the following form:

$$\text{Offset open} \quad Z_{x=0} = 0, \quad \Gamma_x = -e^{-j2\pi \cdot 2x/\lambda}$$

$$\text{Offset covered} \quad Z_{x=0} = \infty, \quad \Gamma_x = +e^{-j2\pi \cdot 2x/\lambda}$$

$$\text{Matched absorber} \quad Z_x = \mathbb{Z}_0, \quad \Gamma_x = 0 .$$

The measurements were performed with various moving offset opens, offset covers, and offset absorbers in 20-cm steps over a range of 2 m. As expected, the measured open and covered reflections are spread out symmetrically over a circle with opposite sign and unity magnitude. The reflection coefficient will rotate clockwise when the offset distance x increases.

The measured absorber reflections are spread out over a circle. This demonstrates that the absorber is not perfectly matched. The radius of this circle is indicative for the remaining reflection (7%), and the center position is indicative of what will be measured on a perfectly matched absorber.

The small offset between the origin and this center is mainly caused by the nonzero imaginary part of the ratio $Z_s/\mathbb{Z}_0$. The delay time in the series absorber has prevented the microphone voltages from perfect interference in the circuit shown in Fig. 4. An adjustable circuit with complex impedances would have eliminated this phase mismatch for distinct frequencies, but will fail to do so over a wide frequency range. Therefore the small offset between zero and the measured reflection is indicative of the measurement accuracy of the experimental setup for small reflections.

3.2 Network Analyzer Bandwidth

To demonstrate the wide usable frequency band, the moduli of Γ_x of a fixed cover, open, and absorber were measured over a frequency range of two decades. For the open and cover, 100% reflection was expected for all frequencies, and 7% reflection was expected for the absorber at 50 Hz (see Section 3.1). It is assumed that below 50 Hz the absorber reflection remains frequency independent. Above this frequency an increase in absorber reflection was observed from VSWR measurements.

As shown in Fig. 6, the measured values are within 5% of the expected values. The network analyzer adjustment procedure described in Section 2.6 has caused a dip in the measured absorber reflection at 50 Hz. A

long-term variation in the mechanical construction (wool density) has misadjusted the 100% reflection calibration point. Improvements in the absorber and its long-term stability, and adjustments at lower frequencies would have improved the overall accuracy.

3.3 Acoustic Loudspeaker Impedance

As mentioned in Section 2.2, the acoustic impedance of a loudspeaker is dependent not only on the acoustic geometry but also on the electrical impedance of the associated amplifier. The cone movements are obstructed by the magnetic field of the induced current. Therefore the lower the electrical impedance, the higher will be the acoustic impedance.

In the acoustic network analyzer this effect was used to reduce the acoustic loudspeaker impedance by means of an associated amplifier with high output impedance. Fig. 7 shows the acoustic impedance of a loudspeaker with open back end and reconstructed from reflection measurements for various electrical load impedances. This demonstrates that for applications as acoustic drivers in network analyzers a significantly higher load

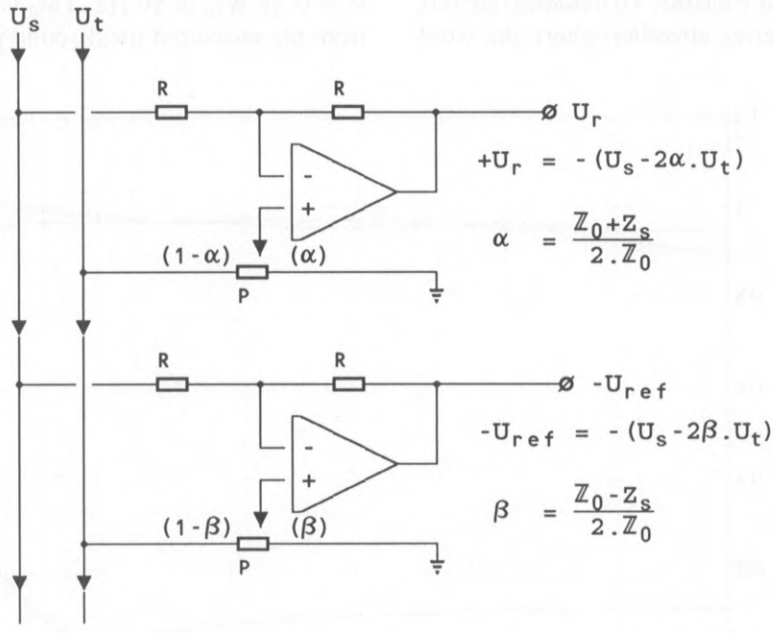

Fig. 4. Simple electronic circuit facilitating signal preprocessing required to obtain reflective and reference voltages.

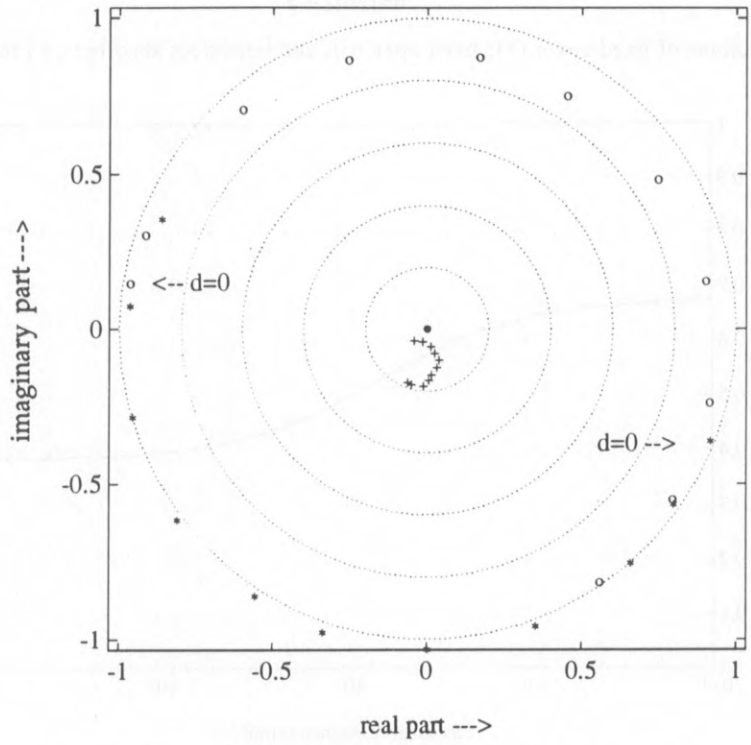

Fig. 5. Measured reflections to various offset covers (*), offset opens (o), and offset absorbers (+) at 50 Hz.

impedance than the nominal impedance (8 Ω) is preferred.

The acoustic impedance is also influenced by the geometry behind the loudspeaker, be it an open tube, absorbing material, or a loudspeaker cabinet. This will be emphasized at the resonating frequencies of the construction. Therefore we think that these types of measurements would be helpful in designing loudspeaker cabinets.

3.4 Nonlinearity Measurements

As mentioned in Section 2.4, turbulent flows in the absorber cause nonlinear transfer. To demonstrate this effect, we realized a series absorber where the wool was highly compressed into one-sixth of the volume used in the network analyzer and packed in a 25-mm-long cylinder of 70-mm diameter. The wool density was adjusted to realize minimum reflections when the back side was left open. Fig. 8 shows the measured reflections when the acoustic power was varied over 40 dB. Above −20-dB source power the reflections from the highly compressed absorber become distorted and dependent on the gas velocity (acoustic power), which indicates turbulent gas flows.

The maximum available acoustic power in the absorber was defined to be 0 dB, which corresponds to $\mathbb{P} = 0.28\ W_{eff}$ at 50 Hz. This value was reconstructed from the measured local sound pressure, the aperture,

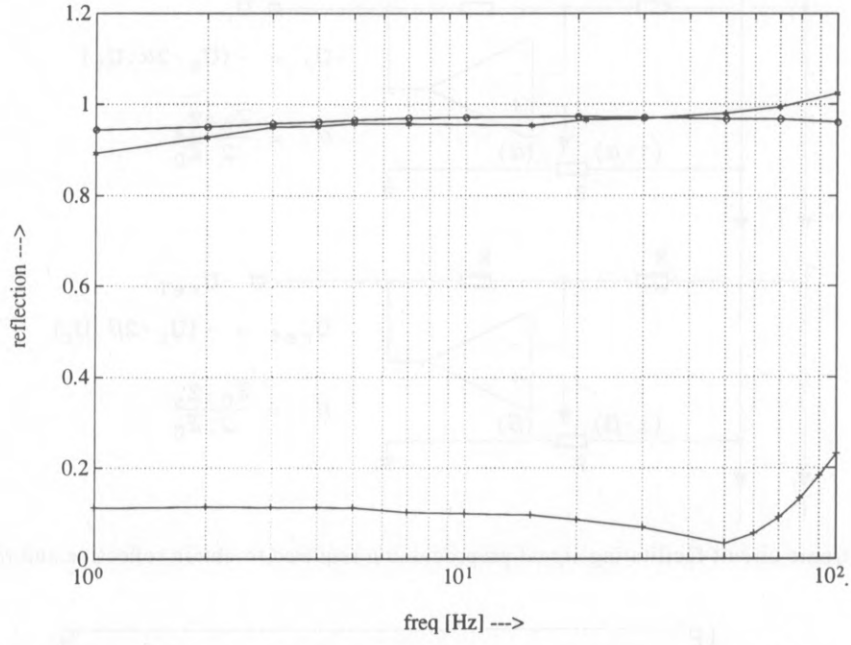

Fig. 6. Measured reflections of fixed cover (*), fixed open (o), and imperfect absorber (+) for various frequencies.

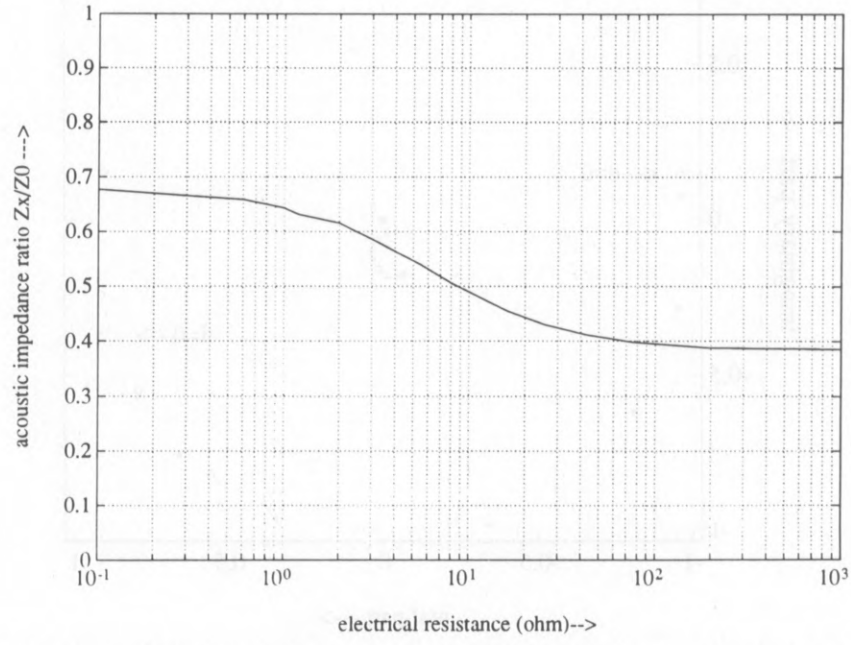

Fig. 7. Acoustic impedance of 8-Ω loudspeaker as a function of electrical source impedance when back end is left open.

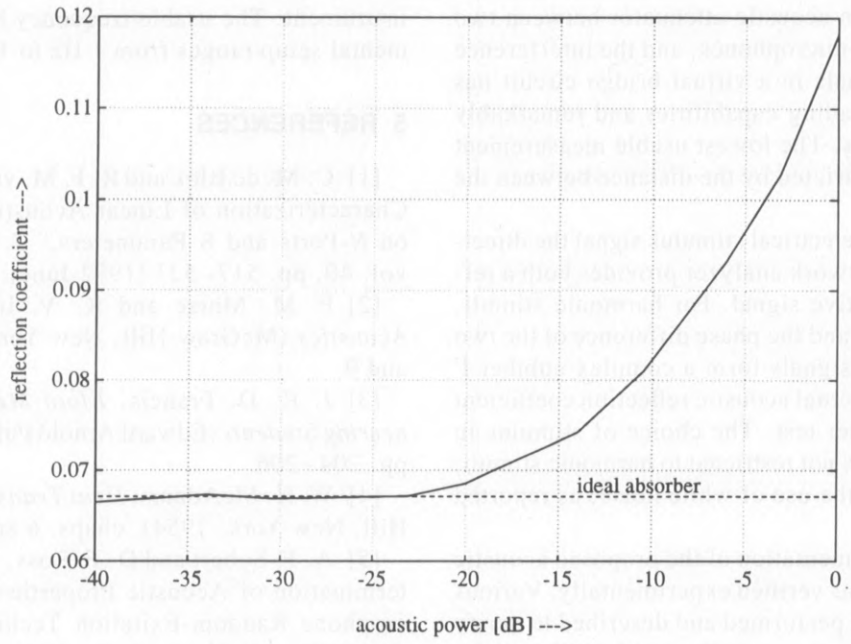

Fig. 8. Measured reflections at 50 Hz versus source power of highly compressed serial absorber.

and the characteristic impedance. The calculated values, based on the measurement of A and p and the relations given in Table 1 are as follows:

A = tube aperture (diameter 0.07 m) = 0.0038 [m^2]

z_0 = specific impedance of free air = 420 [Ns/m^3]

$\mathbb{Z}_0$ = characteristic impedance of tube = $110 \cdot 10^3$ [Ns/m^5]

$\mathfrak{p}$ = local pressure (when homogeneous) = 175 $[N/m^2]_{eff}$

v = local gas velocity (when homogeneous) = 0.42 $[m/s]_{eff}$

p = average sound pressure, $= 1/A \cdot \int\int \mathfrak{p} \cdot dA$ = 175 $[N/m^2]_{eff}$

u = volume flow rate, $= \int\int v \cdot dA$ = 0.0016 $[m^3/s]_{eff}$

$\mathbb{P}$ = acoustic power = 0.28 $[Nm/s]_{eff}$.

To verify the linearity of the built-in absorber of the network analyzer, the reflections to a covered end and an open end were measured for various power levels and appeared to be level independent over the same power range.

4 CONCLUSIONS

We introduced an improved measurement instrument to facilitate reflection measurements on acoustic one-

Table 1. Time-domain relations between elementary acoustic parameters with regard to traveling waves in tubes perfectly terminated with $\mathbb{Z}_0$.

$p(t)$	$\sqrt{(\mathbb{P} \cdot z_0)/A}$	$(\sqrt{\mathbb{P} \cdot \mathbb{Z}_0})$	N/m^2
$u(t)$	$\sqrt{(\mathbb{P}/z_0) \cdot A}$	$(\sqrt{\mathbb{P}/\mathbb{Z}_0})$	m^3/s
$p(t)/u(t)$	z_0/A	$\mathbb{Z}_0$	Ns/m^5
$p(t) \cdot u(t)$	$\mathbb{P}$	$\mathbb{P}$	Nm/s
$\mathbb{P}(t)$	$(p^2/z_0) \cdot A$	$(p^2/\mathbb{Z}_0)$	Nm/s
$\mathbb{P}(t)$	$(u^2 \cdot z_0)/A$	$(u^2 \cdot \mathbb{Z}_0)$	Nm/s

ports. The use of an acoustic attenuator between two fixed wall-mounted microphones, and the interference of microphone signals in a virtual bridge circuit has facilitated direct-reading capabilities and remarkably compact dimensions. The lowest usable measurement frequency is not restricted by the distance between the two microphones.

In response to an electrical stimulus signal the direct-reading acoustic network analyzer provides both a reference and a reflective signal. For harmonic stimuli, the magnitude ratio and the phase difference of the two electrical response signals form a complex number Γ that represents the actual acoustic reflection coefficient of the one-port under test. The choice of stimulus in the proposed setup is not restricted to harmonic stimuli, but also facilitates the use of white noise, as reported in ref [5].

A practical implementation of the proposed acoustic network analyzer was verified experimentally. Various measurements were performed and described to verify the theory and to demonstrate the applicability of the instrument. The usable frequency band of the experimental setup ranges from 1 Hz to 100 Hz.

5 REFERENCES

[1] C. M. de Blok and R. F. M. van den Brink, "Full Characterization of Linear Acoustic Networks Based on *N*-Ports and S Parameters," *J. Audio Eng. Soc.*, vol. 40, pp. 517–523 (1992 June).

[2] P. M. Morse and K. V. Ingard, *Theoretical Acoustics* (McGraw-Hill, New York, 1968), chaps. 6 and 9.

[3] J. R. D. Francis, *Fluid Mechanics for Engineering Students* (Edward Arnold Publ., London, 1975), pp. 204–206.

[4] W. H. McAdams, *Heat Transmission* (McGraw-Hill, New York, 1954), chaps. 6 and 11.

[5] A. F. Sybert and D. F. Ross, "Experimental Determination of Acoustic Properties Using a Two-Microphone Random-Exitation Technique," *J. Acoust. Soc. Am.*, vol. 61, no. 5, pp. 1362–1370 (1977 May).

THE AUTHORS



C. M. de Blok



R. F. M. van den Brink

C. M. (Kees) de Blok was born 1954 July 6. After an electrotechnical education he joined PTT-Research in August of 1971. There he worked in different telecommunication areas, such as audio/video transmission, scribofonie, and digital filters, until 1978. He then became involved with the development of measuring and installation methods for the first direct detection optical fiber links in The Netherlands. In this field he gained two patents: one for a directional coupler; another for a fiber alignment system. He was also coauthor of a publication on fiber installation.

Since 1984 he has worked on the development and realization of different coherent optical links and has been coauthor of a few conference proceedings on distribution and subscriber networks.

In addition to his work at PTT-Research, in 1985 he started research on thermoacoustic energy conversion. He is now working with others on modeling the complete thermoacoustic process.

•

R. F. M. (Rob) van den Brink was born 1955 May 21. He graduated in 1984 from the Technical University Delft, in The Netherlands, with a degree in electrotechnical engineering. His graduation project concerned the development of feeds for microwave antennas. He joined the same university to work on microwave remote sensing experiments.

In 1985 he joined PTT-Research in The Netherlands and since then has worked on fiber-optical transmission systems. He developed wideband optical receivers and transmitters operating up to a few GHz, and various new measurement and software design tools for optoelectronic circuits. His group designed various analog key circuits for coherent optical transmission systems, both for internal projects and for an ESPRIT (UCOL) project supported by the EEC.

Currently he is working for his thesis on a systematic design approach for wideband analog circuits, applied to high-performance optical receivers. His approach is extensively based on measurements of the key components in a circuit, postprocessing on the measured raw data, parameter extraction, and computer simulation.